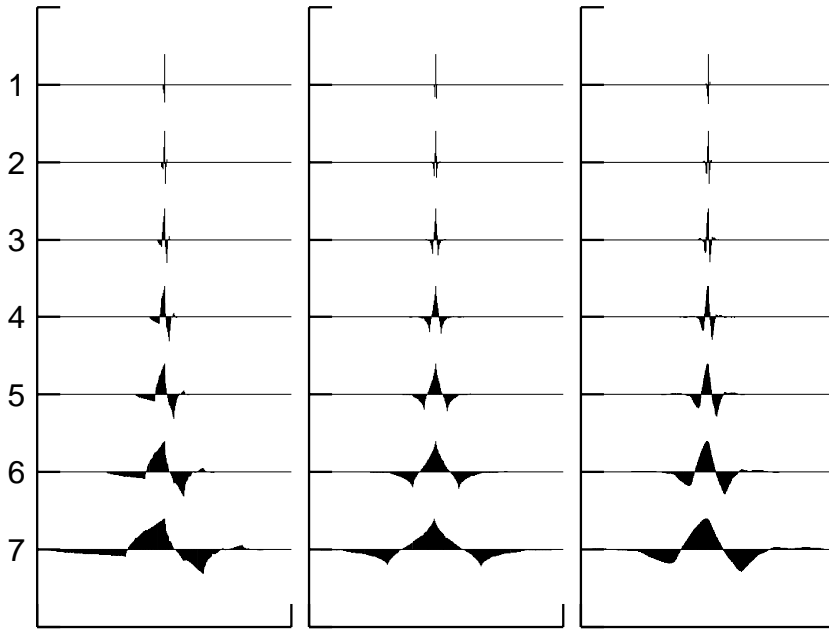
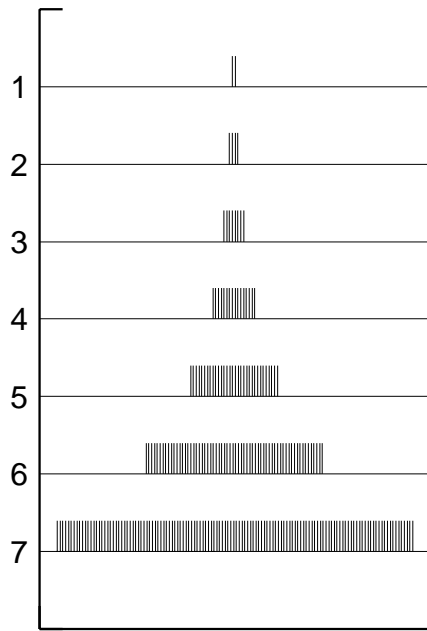


**Figure 1.** Haar wavelet filters for scales  $\tau_j = 2^{j-1}$ ,  $j = 1, 2, \dots, 7$ .



**Figure 2.** D(4), C(6) and LA(8) wavelet filters for scales  $\tau_j = 2^{j-1}$ ,  $j = 1, 2, \dots, 7$ .



**Figure 3.** Haar scaling filters for scales  $\lambda_{J_0} = 2^{J_0}$ ,  $J_0 = 1, 2, \dots, 7$ .

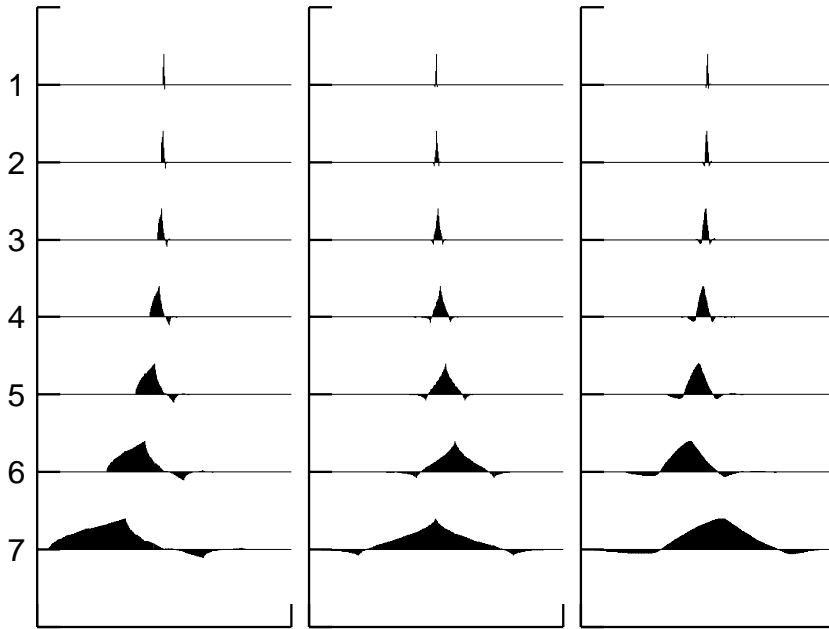


**Figure 4.** D(4), C(6) and LA(8) scaling filters for scales  $\lambda_{J_0} = 2^{J_0}$ ,  $J_0 = 1, 2, \dots, 7$ .

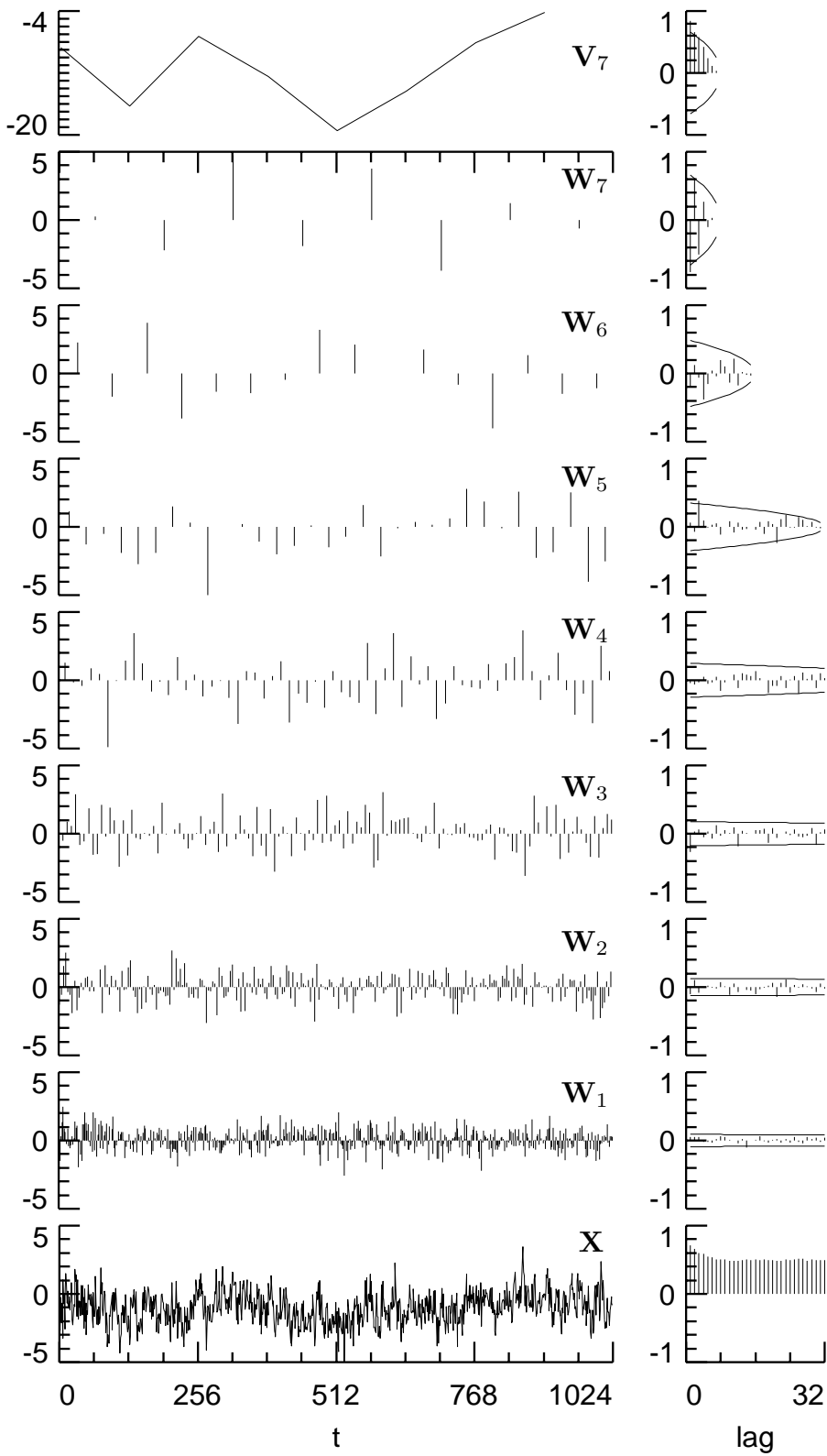


**Figure 5.** LA(8) DWT coefficients for simulated FD(0.4) time series and sample ACSs.

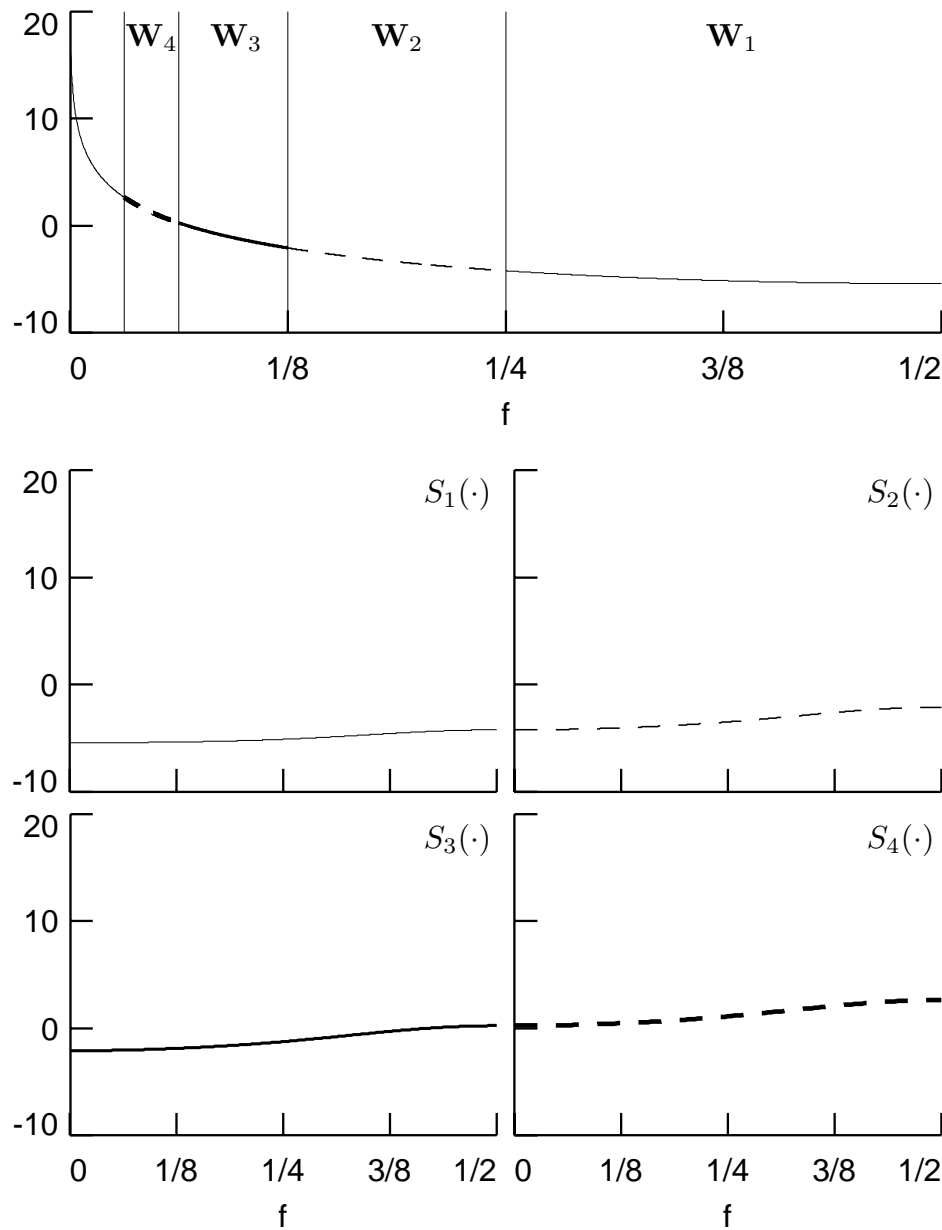


**Figure 6.** SDFs for an FD(0.4) process (top plot) and for nonboundary LA(8) wavelet coefficients in  $\mathbf{W}_1$ ,  $\mathbf{W}_2$ ,  $\mathbf{W}_3$  and  $\mathbf{W}_4$ . The vertical axes are all in units of decibels (i.e., we plot  $\log_{10}(S_X(f))$  versus  $f$ ). The vertical lines in the top plot denote the nominal pass-bands for the four  $\mathbf{W}_j$ .

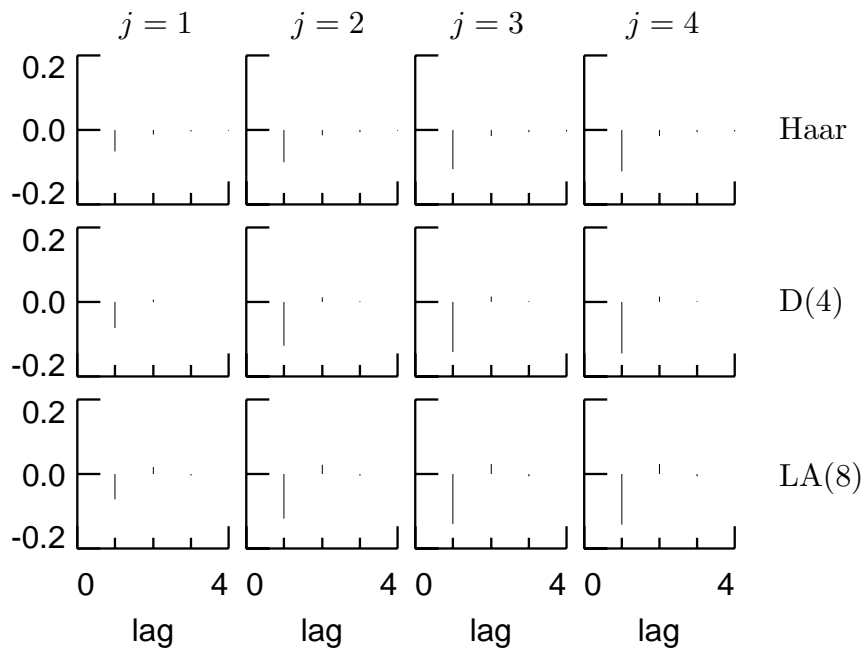


**Figure 7.** ACSs at  $\tau = 1, \dots, 4$  for Haar, D(4) and LA(8) wavelet coefficients  $W_{j,t}$ ,  $j = 1, \dots, 4$ , of an FD(0.4) process. The ACS values are plotted as deviations from zero (some are not visible because they are so close to zero).

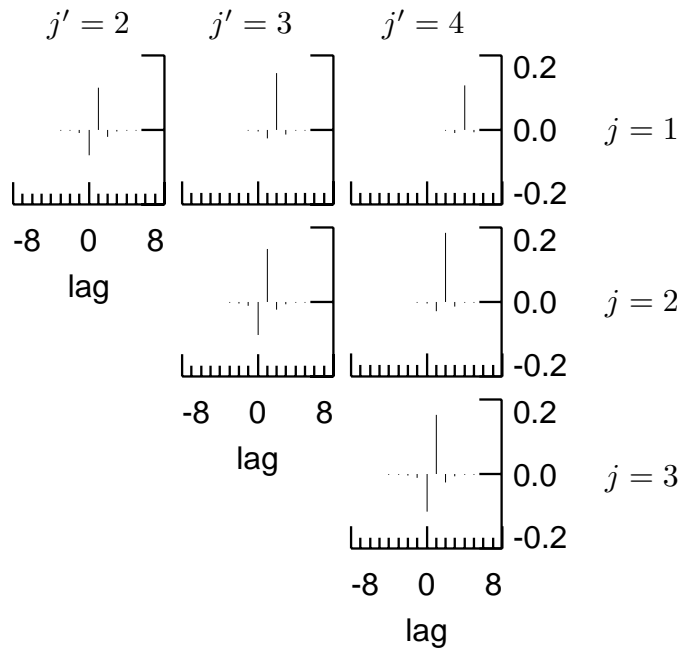


**Figure 8a.** Correlation between the Haar wavelet coefficients  $W_{j,t}$  and  $W_{j',t'}$  formed from an FD(0.4) process and for levels satisfying  $1 \leq j < j' \leq 4$ .

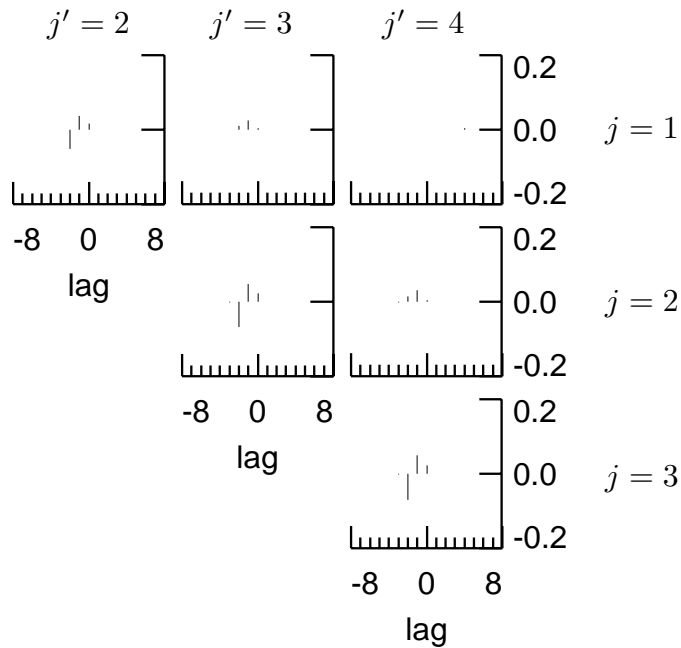


**Figure 8b.** As in Figure 8a, but now using the LA(8) DWT.



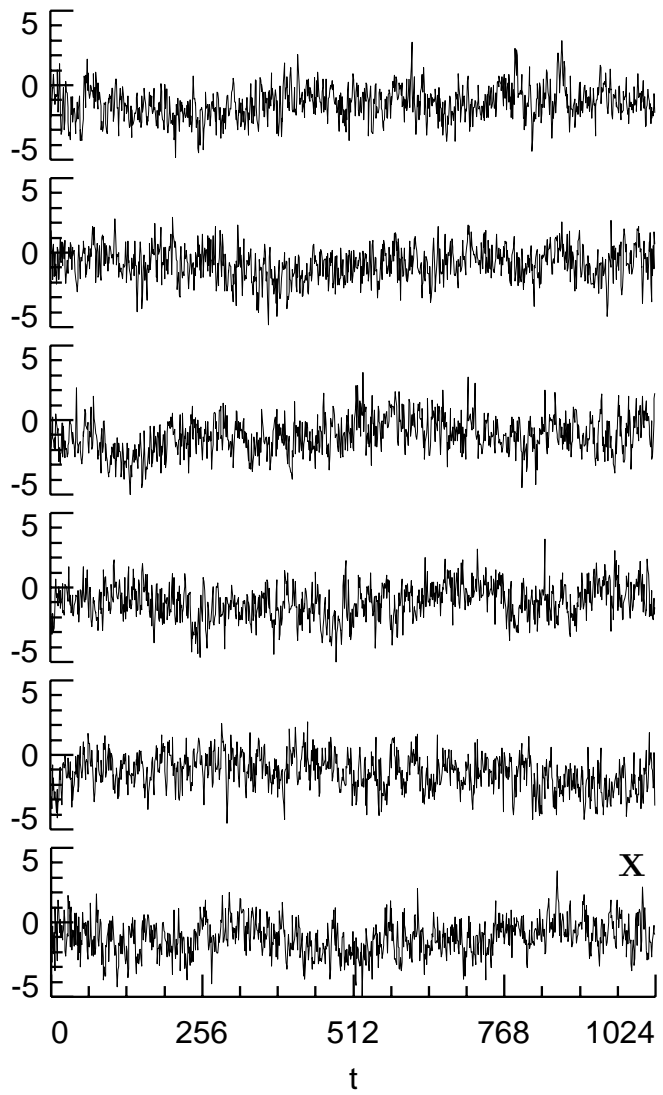


**Figure 9.** Simulated FD(0.4) time series  $\mathbf{X}$  of Figure 5 (bottom panel), above which are five series that were bootstrapped from  $\mathbf{X}$  using an LA(8) DWT.

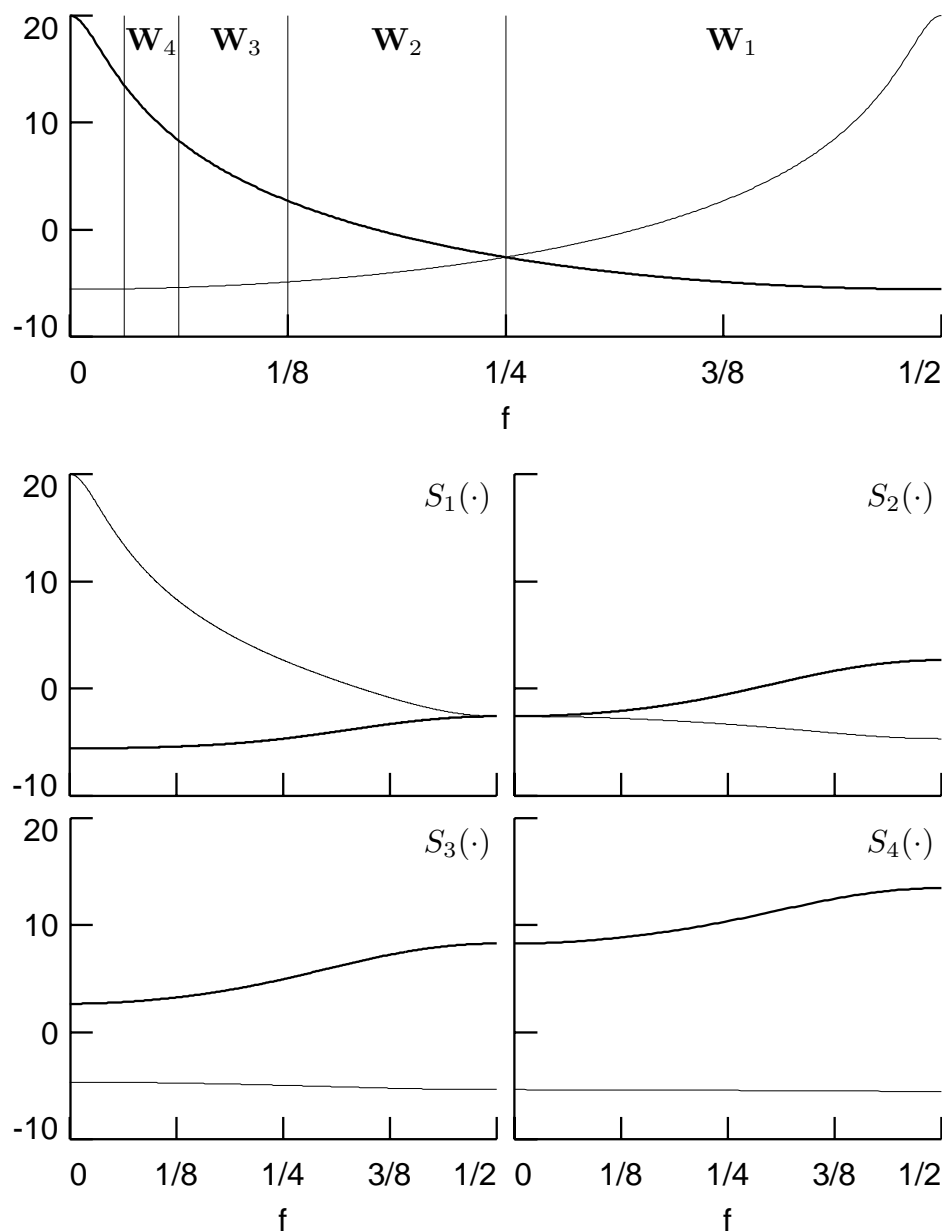


**Figure 10.** SDFs for AR(1) processes (top plot) with  $\phi = 0.9$  (thick curve) and  $-0.9$  (thin) and for corresponding nonboundary LA(8) wavelet coefficients in  $\mathbf{W}_1$  to  $\mathbf{W}_4$  (bottom four plots). The vertical axes are in decibels, and the vertical lines in the top plot denote the nominal pass-bands for the four  $\mathbf{W}_j$ .

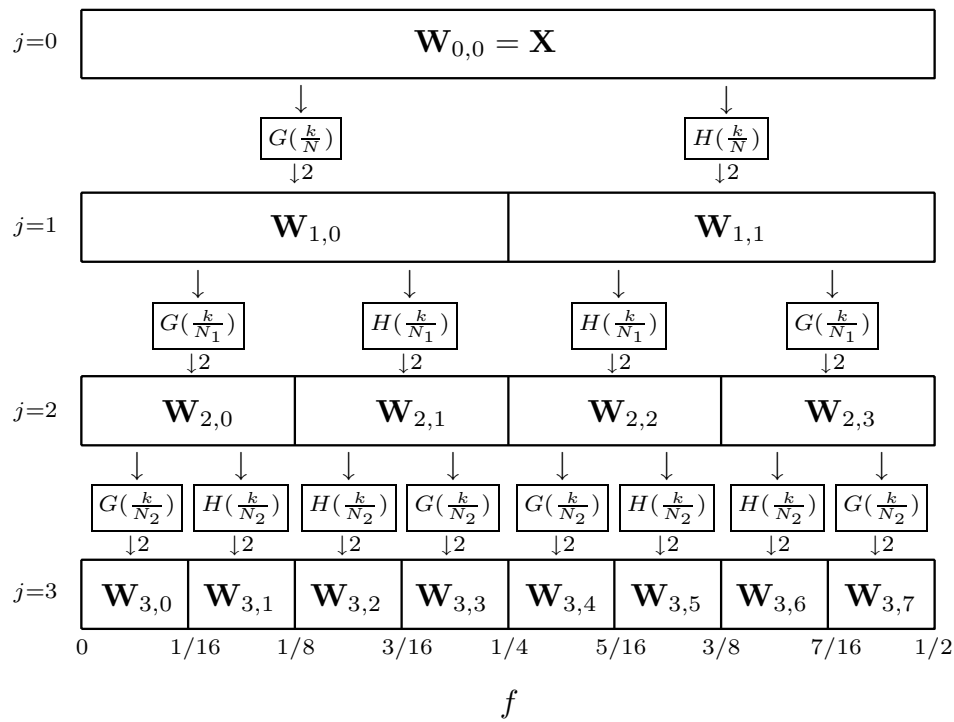


**Figure 11.** Flow diagram illustrating the analysis of  $\mathbf{X}$  into  $\mathbf{W}_{3,0}, \dots, \mathbf{W}_{3,7}$  (recall that  $N_j \equiv N/2^j$ ).

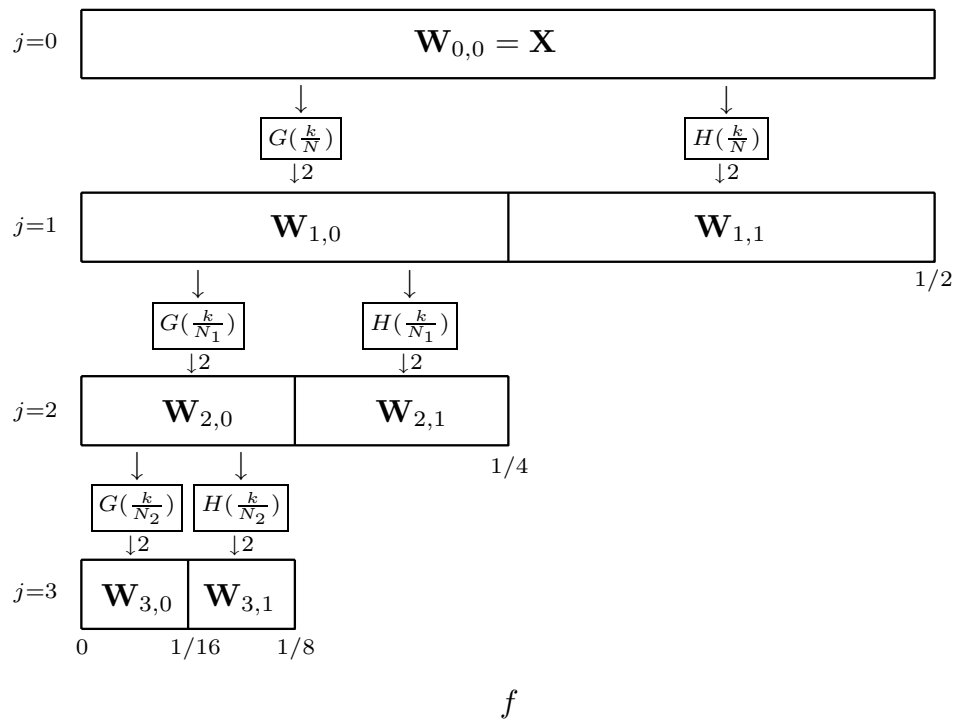


**Figure 12.** Flow diagram illustrating the analysis of  $\mathbf{X}$  into  $\mathbf{W}_{3,0}$ ,  $\mathbf{W}_{3,1}$ ,  $\mathbf{W}_{2,1}$  and  $\mathbf{W}_{1,1}$ , which is identical to a partial DWT of level  $J_0 = 3$ .

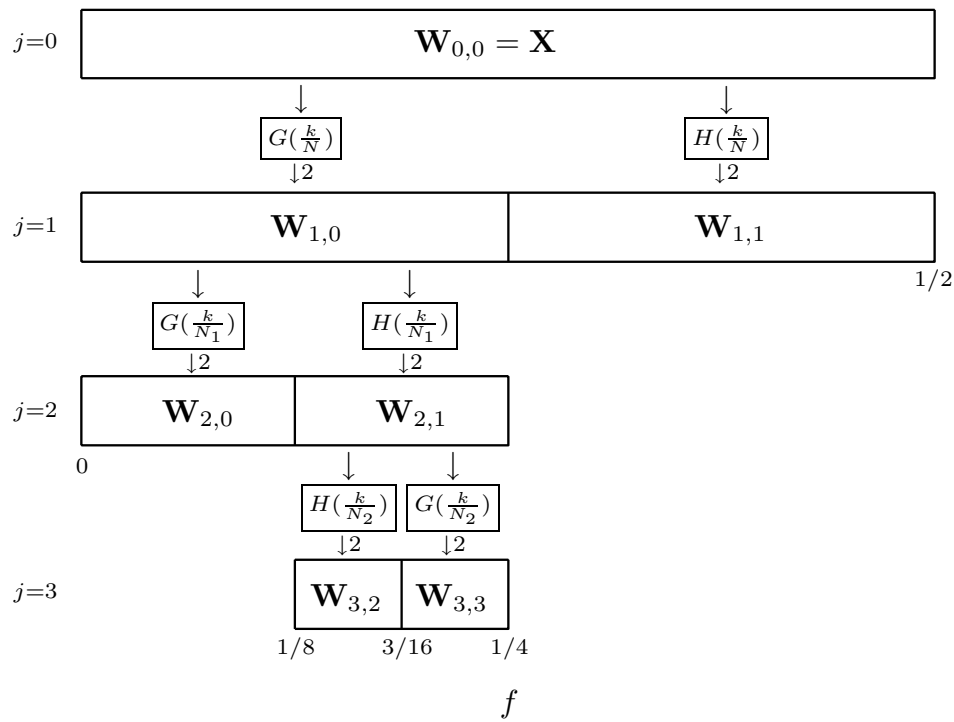


**Figure 13.** Flow diagram illustrating the analysis of  $\mathbf{X}$  into  $\mathbf{W}_{2,0}$ ,  $\mathbf{W}_{3,2}$ ,  $\mathbf{W}_{3,3}$  and  $\mathbf{W}_{1,1}$ , an arbitrary disjoint dyadic decomposition.